Title
Optical theorem and the inversion of cross section data for atom scattering from defects on surfaces

Journal
The Journal of Chemical Physics, 102(17)

ISSN
0021-9606

Authors
Hamburger, DA
Gerber, RB

Publication Date
1995-05-01

DOI
10.1063/1.469129

Optical Theorem and the Inversion of Cross Section Data for Atom Scattering from Defects on Surfaces

D.A. Hamburger[a,b] and R.B. Gerber[b,c]

[a] *Department of Physics, The Hebrew University of Jerusalem, Jerusalem 91904, Israel*

[b] *The Fritz Haber Center for Molecular Dynamics, The Hebrew University of Jerusalem, Jerusalem 91904, Israel*

[c] *Department of Chemistry, University of California - Irvine, Irvine, CA 92717, USA*

Abstract

The information content and properties of the cross section for atom scattering from a defect on a flat surface are investigated. Using the Sudden approximation, a simple expression is obtained that relates the cross section to the underlying atom/defect interaction potential. An approximate inversion formula is given, that determines the shape function of the defect from the scattering data. Another inversion formula approximately determines the potential due to a weak corrugation in the case of substitutional disorder. An Optical Theorem, derived in the framework of the Sudden approximation, plays a central role in deriving the equations that conveniently relate the interaction potential to the cross section. Also essential for the result is the equivalence of the operational definition for the cross section for scattering by a defect, given by Poelsema and Comsa, and the formal definition from quantum scattering theory. This equivalence is established here. The inversion result is applied to determine the shape function of an Ag atom on Pt(111) from scattering data.

I. INTRODUCTION

The pioneering work by Poelsema, Comsa and coworkers [1–5] on atom-surface scattering in the last decade, has led to the introduction and application of the concept of the cross section of a defect on a surface in studies of questions related to surface disorder. Extensive experimental work in the field (as summarized in ref. [6]) has focused primarily on the measurement of the dependence of the cross section on the surface parameters, usually the coverage dependence. Some efforts have also been directed to the dependence on the scattering parameters, such as incidence energy and angle. These cross section studies have attracted significant theoretical interest, [7–14] concentrating almost exclusively on the dependence on the scattering parameters. Relatively little attention has been paid to the inverse question of the *information content* of the cross section. Most work in this direction has been experimental, again focusing on the use of cross section data to study *coverage-dependent* questions, such as the onset of Ostwald ripening, [15] and whether growth proceeds in a layer-by-layer fashion. [16–21] With very few exceptions, [14,22] most studies to date do not deal with the issue of the *structural* information contained in the cross section. For instance, can the cross section be used to extract the shape of an object on the surface, or its electron density profile? Can the interaction potential between an atom and a surface defect be obtained from the cross section data? In the present paper, we address these questions theoretically, by focusing on what can be learned from studying the cross section of an *individual* defect on a surface.

To make contact with experiment, through the operational definition of the cross section proposed by Poelsema and Comsa, [6] it is required to show the equivalence of the latter definition to the standard formal one from scattering theory, which we shall employ. Here we will establish this equivalence. An analytical study of the cross section is most easily performed by relating the cross section through an optical theorem to the scattering amplitude. This has been done by several authors. [18,7,9] We derive an optical theorem for atom-surface scattering by use of the Sudden Approximation (SA), [23] which has two sig-

nificant advantages: it leads to a simple explicit form for the cross section, and is expected to be fairly accurate, as the SA performs best for the calculation of specular amplitudes. By employing our optical theorem result, we will answer a number of specific questions related to the information that can be extracted from the single defect cross section.

First we shall examine the relative role of the long range dispersion forces *vs* the short range repulsive part of the potential in determining the interaction of a He atom with an adsorbed defect. It is a well-recognized fact in surface scattering theory, [24,7,11,6] that the magnitude of the total cross section of a defect is dominated by small angle deflections caused by the long range forces. We will show that they are mostly effective in setting the magnitude of the cross section, whereas at least for the high-energy regime the short-range forces tend to determine its qualitative shape.

A second issue that will be pursued is whether the cross section be used to perform an inversion of the He-defect interaction potential. An affirmative answer will be given in two important cases: the cross section can be used to invert the semiclassical *shape function* of a defect on a surface, and to approximately invert the interaction potential of a He atom with a weak corrugation, e.g., due to dilute substitutional disorder. The results are applied to obtain the shape function of an Ag atom on Pt(111), using cross section data from P. Zeppenfeld. [25]

The structure of the article is as follows: we discuss the standard and operational definitions of the cross section in section II, and prove their equivalence. In section III, we briefly review the SA, and derive the optical theorem for atom-surface scattering within the SA. We then proceed to discuss a number of applications of the optical theorem, in section IV The first is a discussion of the influence of the short range repulsive part of the atom-surface interaction potential. The second is perhaps the central result of this paper: an inversion scheme for the shape function of an adsorbate on a surface from cross section measurements. We apply this result to data for Ag/Pt(111). The third application is the approximate inversion of the potential from the cross section data. Concluding remarks are presented in section V

II. DEFINITION OF THE CROSS SECTION

Consider a scattering experiment of an atom beam with wave-vector $\mathbf{k} = (k_x, k_y, k_z)$, impinging on a flat surface (the $z = 0$ plane). Let $\mathbf{R} = (x, y)$ denote a vector in the plane. A typical experimental setup will involve a highly monochromatic beam with a lateral spread in the surface plane. This beam is suitably described by a set of states $|\Psi_{in}\rangle = |\Phi_{\mathbf{R}}\rangle$. After impinging upon the surface, the beam is scattered, in part by the defect whose cross section we are interested in. To derive the cross section, we start from the definition of the quantum differential scattering cross section (QDCS) for two-body collisions. [26] This definition generalizes quite naturally for atom-surface scattering, as we will demonstrate. Let $w(d\Omega \leftarrow \Phi_{\mathbf{R}})$ denote the probability that a particle incident upon a target as a wave packet Φ, displaced laterally by $\mathbf{R}$ with respect to the origin, emerges after an elastic collision in the solid angle $d\Omega$. Then the average number of observed scatterings into $d\Omega$ is:

$$N_{sc}(d\Omega) = \sum_i w(d\Omega \leftarrow \Phi_{\mathbf{R}_i}) \approx \int d^2R\, n_{inc} w(d\Omega \leftarrow \Phi_{\mathbf{R}})$$

where n_{inc} is the incident density, which we assume to be uniform over an area A, i.e., $n_{inc} = N_{inc}/A$, so that:

$$N_{sc}(d\Omega) = \frac{N_{inc}}{A}\frac{d\sigma}{d\Omega}d\Omega \tag{1}$$

where $d\sigma/d\Omega$ is the differential cross section, defined as:

$$\frac{d\sigma}{d\Omega}d\Omega \equiv \sigma(d\Omega) = \int_A d^2R\, w(d\Omega \leftarrow \Phi_{\mathbf{R}}) \tag{2}$$

Thus, as is well known, the QDCS is seen to be a measure of the target area effective in scattering the incident beam. It must be emphasized that the definition of the QDCS excludes the forward direction. Classically speaking, the reason is that one cannot distinguish a forwardly scattered particle from one that did not interact with the target at all. The analogue in surface scattering from a defect, is that one cannot distinguish a *specularly* scattered particle from one that was scattered by the flat part of the surface. More formally, the reason

is that inclusion of the forward direction would lead to a divergence of the cross section. We would now like to discuss the connection between the latter definition, which is widely accepted for two-body processes, and the operational definition proposed by Poelsema and Comsa [6] for atom-surface scattering, and applied extensively for cross section calculations from diffraction data. Their formula reads:

$$\Sigma_{op} = -\lim_{n\to 0} \frac{1}{I_0}\frac{dI_s}{dn} \tag{3}$$

where Σ_{op} is the *total* scattering cross section, I_s, I_0 represent the specular scattering intensity from the corrugated and flat (smooth, defect-free) surfaces respectively, and n is the number of defects per total surface area. Xu *et al.* [10] employed this formula to derive an expression for the cross section based on Gaussian wave packets, and showed that their expression can be interpreted as an optical theorem. We will show that the operational definition (eq.(3)), is in fact *identical* to the standard definition of quantum scattering theory (eq.(2)), without recourse to a specific method of calculating the quantities that appear in the formulas. This is true, provided the proper conditions are established to relate two-body and atom-surface collisions. The conditions under which the QDCS is defined, are: [26]

- the incident particles have a sharply defined momentum $\mathbf{p}_0$ and are randomly displaced in a plane perpendicular to $\mathbf{p}_0$,
- the distribution of scatterers must be such as to avoid coherent scattering off two or more centers.

When interpreted in terms of atom-surface scattering, we see that the first condition may be traded by random lateral displacements parallel to the surface plane (maintaining a sharply peaked momentum). The second requires that the defects are distributed very dilutely. This is, however, exactly the assumption underlying the operational definition, and of course holds for scattering off a *single* defect. Thus the conditions assumed for the definition of the two-body cross section are naturally extendible to the atom-surface case, and suit the operational definition. In order to demonstrate the equivalence of the

definitions, we first replace $N_{sc}(\Omega)/N_{inc}$ by $I(d\Omega)/I_0\, d\Omega$ in eq.(1), where I is the *off*-specular intensity. I_0 is the incident intensity, which is clearly equal to the total scattered intensity in the case of a *flat* surface, and is hence indeed the same quantity as defined in the discussion of the operational definition above. With these replacements, the total cross section is:

$$\Sigma \equiv \int \frac{d\sigma}{d\Omega}\, d\Omega = \frac{A}{I_0} \int I(\Omega)\, d\Omega \tag{4}$$

Next consider taking the limit in the operational definition. This can be done by assuming that only one defect is present on the surface, so that for all practical purposes $dn = 1/A$, A being the total surface area, and $dI = I_s - I_0$. Then from eq.(3):

$$\Sigma_{op} = \frac{A}{I_0}(I_0 - I_s) \tag{5}$$

But clearly, $I_0 - I_s = \int I(\Omega)\, d\Omega$, so that $\Sigma_{op} = \Sigma$, as claimed.

III. OPTICAL THEOREM FOR SURFACE SCATTERING IN THE SUDDEN APPROXIMATION

We very briefly review the SA. For more details see e.g. the review by Gerber. [23]

A. The Sudden Approximation

Basically, the SA requires that the momentum transfer in parallel to the surface be small compared with the momentum transfer normal to the surface, i.e. [27,28]

$$|\mathbf{q}' - \mathbf{q}| \ll 2k_z \tag{6}$$

where k_z is the incident wave number in the z direction, $\mathbf{q}$ is the incident wave vector in parallel to the surface plane, and $\mathbf{q}'$ is any intermediate or final wave vector in parallel to the surface plane which plays a significant role in the scattering process. The S-matrix element for scattering from $\mathbf{q}$ $\mathbf{q}'$ may then be shown to be given by the function:

$$\langle \mathbf{q}|S|\mathbf{q}'\rangle = \frac{1}{A}\int_{\text{surf}} d\mathbf{R}\, e^{2i\eta(\mathbf{R})}\, e^{i\Delta\mathbf{q}\cdot\mathbf{R}} \tag{7}$$

where $\mathbf{R} = (x, y)$ and $\eta(\mathbf{R})$ is the scattering phase shift computed for fixed $\mathbf{R}$, given in the WKB approximation by:

$$\eta(\mathbf{R}) = \int_{z_t(\mathbf{R})}^{\infty} dz \left[\left({k_z}^2 - \frac{2\,m\,V(\mathbf{R}, z)}{\hbar^2} \right)^{\frac{1}{2}} - k_z \right] - k_z\, z_t(\mathbf{R}) \tag{8}$$

Here $z_t(\mathbf{R})$ is the classical turning point for the integrand in eq.(8). The normalization is chosen such that the unit-cell A is the average area available for one adsorbate, i.e, is determined by the coverage. This choice is suitable for low coverages, when the simultaneous interaction of a He atom with two neighboring adsorbates is small. Of course, an adsorbate may "spill over" beyond its unit-cell due to the long range of the potential, and hence the integration in eq.(7) is over the entire surface. Condition (6) for the validity of the Sudden approximation is expected to break down for systems of high corrugation. For instance, certain isolated adsorbates on an otherwise flat surface can represent, for realistic parameters, a very substantial local corrugation. Nevertheless, previous calculations have shown that the Sudden approximation reproduces rather well many features of the scattering from isolated adsorbates. [29] Features for which it breaks down are, e.g, intensity peaks due to double collision events, in which the incoming atom first hits the surface and then the adsorbate (or vice versa), which are a particularly sensitive manifestation of a strong corrugation (we note that a double-collision version of the Sudden approximation has recently been developed [30]). However, due to the assumption (6), the Sudden approximation is particularly useful for the evaluation of specular intensities at incidence angles close to the specular direction, as confirmed by comparison with numerically exact wave packet calculations. [11] In the context of the present work, only the specular intensities are required (which are obtained by setting $\mathbf{q}' = \mathbf{q}$ in eq.(7)), which constitutes the most favorable condition for the Sudden.

B. Derivation of the Optical Theorem

The ensuing discussion closely follows that of Taylor [26] for two-body scattering. We proceed to derive the optical theorem for surface scattering within the SA.

The probabilities $w(d\Omega \leftarrow \phi_{\mathbf{R}})$ in eq.(2) are:

$$w(d\Omega \leftarrow \Psi_{in}) = d\Omega \int_0^\infty p^2 dp \, |\Psi_{out}(\mathbf{p})|^2 \qquad (\mathbf{p} = \hbar\mathbf{k}) \tag{9}$$

since $w(d^3p \leftarrow \Psi_{in}) = d^3p \, |\Psi_{out}(\mathbf{p})|^2$ is the probability that long after the collision the particle incident as Ψ_{in}, emerging as Ψ_{out}, has momentum in $(\mathbf{p}, \mathbf{p}+d\mathbf{p})$. Only the direction of $\mathbf{p}$ is of interest, as we are assuming elastic scattering. The "in" and "out" states are related by the S-matrix: $|\Psi_{out}\rangle = S \, |\Psi_{in}\rangle$. In the momentum representation:

$$\Psi_{out}(\mathbf{p}) = \int d^3p' \, \langle \mathbf{p}|S|\mathbf{p}'\rangle \, \Psi_{in}(\mathbf{p}') \tag{10}$$

The combination of eqs.(2,9-10) yields the differential cross section. Following the discussion in the preceding section, it can be seen that there is nothing which essentially restricts the use of eqs.(2,9-10) to two-body scattering, and with the restriction of scattering angles to the half-space above the surface ($z > 0$), they may as well be applied to atom-surface scattering. We now proceed to calculate the differential cross section within the Sudden approximation. Let us denote $\mathbf{p} = \hbar(\mathbf{q}, k_z)$, where $\mathbf{q}$ is the wave-vector component in parallel to the surface, and $\Delta\mathbf{q} \equiv \mathbf{q}' - \mathbf{q}$. We require the familiar "scattering-amplitude" f, in terms of which the Optical Theorem will be expressed. To find its form within the SA, we first write down a general expression for the S-matrix element, in the case of scattering from a surface with a defect. This expression must be composed of two terms, reflecting specular (the analogue of forward scattering in the gas phase) and off-specular scattering. The first arises in the case of scattering from the flat part of the surface, whereas the second is due to scattering from the defect. Energy is assumed to be conserved, so the general expression for the S-matrix element $\langle \mathbf{p}|S|\mathbf{p}'\rangle$ contains an on-shell delta-function of the energy $E_p \equiv p^2/2m$:

$$\langle \mathbf{p}|S|\mathbf{p}'\rangle = \delta(p_z + p_z') \, \delta(\hbar\Delta\mathbf{q}) + \frac{i}{2\pi m\hbar}\delta(E_p - E_{p'}) f(\mathbf{p} \leftarrow \mathbf{p}') \tag{11}$$

The identification of the scattering-amplitude by comparing eqs.(7),(11) is now made as follows. First, the phase-shift η is constant for scattering from a flat surface, and may well be chosen zero. In this case the SA yields $\langle \mathbf{q}|S|\mathbf{q}'\rangle = \delta(\Delta\mathbf{q})$ (eq.(7) with $\eta(\mathbf{R}) = 0$), in agreement with the general form for specular scattering. Second, we consider the remainder after subtraction of the specular part from the RHS of eq.(7):

$$g(\mathbf{q} \leftarrow \mathbf{q}') = \frac{2\pi}{iA} \int_{\text{surf}} d\mathbf{R} \, \left(e^{2i\eta(\mathbf{R})} - 1 \right) e^{i\Delta\mathbf{q}\cdot\mathbf{R}} \tag{12}$$

so that:

$$\langle \mathbf{q}|S|\mathbf{q}'\rangle = \frac{1}{A}\delta(\Delta\mathbf{q}) + \frac{i}{2\pi} g(\mathbf{q} \leftarrow \mathbf{q}') \tag{13}$$

Energy conservation is implicitly assumed in the SA expression eq.(7). Still, comparing eq.(13) and eq.(11), g is not quite the scattering amplitude yet, since it does not include the action of the S-matrix on the wave-function part in perpendicular to the surface. The SA derivation [27] yields only the action on the part parallel to the surface. However, we can obtain the corresponding factor by comparison to the well known partial-wave expansion result. If we assume a plane wave He-beam at normal incidence to a perfectly flat surface with a spherically symmetric He-adsorbate interaction, the partial-wave expansion conditions apply. The gas-phase expression for the scattering amplitude is then: [26]

$$f(\mathbf{k} \leftarrow \mathbf{k}') = \frac{2\pi}{ik} \sum_{l,m} Y_l^m(\hat{\mathbf{k}}) \left[e^{2i\delta_l(E_p)} - 1 \right] Y_l^m(\hat{\mathbf{k}}')^* \tag{14}$$

where $Y_l^m(\hat{\mathbf{k}})$ is the spherical harmonic whose argument $\hat{\mathbf{k}}$ denotes the polar angle (θ, ϕ) of $\hat{\mathbf{k}}$, and $\delta_l(E_p)$ is the phase-shift in the angular momentum basis $\{|E, l, m\rangle\}$. Comparing eqs.(12),(14), we see that the contribution of the component perpendicular to the surface is a factor of $1/k$, so that the SA scattering amplitude is:

$$f(\mathbf{p} \leftarrow \mathbf{p}') = \frac{1}{k} g(\mathbf{q} \leftarrow \mathbf{q}') \tag{15}$$

We emphasize at this point our strategy for deriving the optical theorem: the analogue to the gas-phase forward *vs* non-forward scattering, is the flat-surface *vs* defect scattering. Within the SA, this distinction is easily made by separating the vanishing part from the non-zero part of the phase-shift.

We are now ready to calculate the differential cross section within the SA. Substituting eq.(11) into eq.(10) yields:

$$\Psi_{out}(\mathbf{p}) = \Psi_{in}(\mathbf{q}, -k_z) + \frac{i}{2\pi m\hbar} \int d^3p' \, \delta(E_p - E_{p'}) \, f(\mathbf{p} \leftarrow \mathbf{p}') \, \Psi_{in}(\mathbf{p}') \tag{16}$$

The first term is the wave scattered from the flat part of the surface, the second by the defect. Next we restrict observation to defect scattering only. Using the lateral displacement assumption from section II we then obtain:

$$\Psi_{out}(\mathbf{p}) = \frac{i}{2\pi m\hbar}\int d^3p'\,\delta(E_p - E_{p'})\,f(\mathbf{p}\leftarrow\mathbf{p}')\,e^{-\frac{i}{\hbar}\mathbf{R}\cdot\mathbf{p}'}\Phi(\mathbf{p}') \tag{17}$$

Substituting eq.(17) into eq.(9) and then into (2):

$$\begin{aligned}\sigma(d\Omega) = \frac{d\Omega}{2\pi m^2\hbar^2}\int_A d^2R\int_0^\infty p^2\,dp\ \times\\ \int d^3p'\,\delta(E_p - E_{p'})\,f(\mathbf{p}\leftarrow\mathbf{p}')\,e^{-\frac{i}{\hbar}\mathbf{R}\cdot\mathbf{p}'}\Phi(\mathbf{p}')\ \times\\ \int d^3p''\,\delta(E_p - E_{p''})\,f^*(\mathbf{p}\leftarrow\mathbf{p}'')\,e^{\frac{i}{\hbar}\mathbf{R}\cdot\mathbf{p}''}\Phi(\mathbf{p}'')\end{aligned} \tag{18}$$

The $\mathbf{R}$ integration yields $(2\pi)^2\,\delta(\mathbf{q}'' - \mathbf{q}')$. It is easily checked, using some well known properties of the delta-function, that consequently:

$$\int d^2R\,e^{\frac{i}{\hbar}\mathbf{R}\cdot(\mathbf{p}''-\mathbf{p}')}\,\delta(E_p - E_{p'})\,\delta(E_p - E_{p''}) = (2\pi)^2\frac{m\,\hbar}{k'_z}\delta(\mathbf{p}'' - \mathbf{p}')\,\delta(E_p - E_{p'}) \tag{19}$$

Inserting this into eq.(18) and applying the momentum delta-function, we obtain:

$$\sigma(d\Omega) = \frac{\hbar d\Omega}{m\hbar}\int_0^\infty p^2dp\int d^3p'\,\frac{1}{k'_z}\delta(E_p - E_{p'})\,|g(\mathbf{q}\leftarrow\mathbf{q}')|^2\,|\Phi(\mathbf{p}')|^2\frac{1}{(k')^2} \tag{20}$$

Next we use $\delta(E_p - E_{p'}) = \frac{m}{p}\delta(p - p')$ to do the radial integration over p:

$$\sigma(d\Omega) = d\Omega\int d^3p'\,\frac{1}{k'_z\,k'}\,|g(\mathbf{q}\leftarrow\mathbf{q}')\,\Phi(\mathbf{p}')|^2 \tag{21}$$

where $|\mathbf{p}| = |\mathbf{p}'|$. To simplify the last integral and obtain the standard form, we recall that Φ represents the incident wave-function (at zero lateral displacement). The simplification is obtained by the physically plausible assumption that Φ is *sharply peaked* about the incidence momentum $\mathbf{p}_0$. More quantitatively, we assume that $\frac{1}{k'_z\,k'}g(\mathbf{q}\leftarrow\mathbf{q}')$ does not vary appreciably in the region of Φ's peak, so that it can be taken outside of the integral sign, and be replaced by its values at $\mathbf{k}_0$. Using further the normalization condition $\int d^3p'\,|\Phi(\mathbf{p}')|^2 = 1$, we finally obtain the familiar looking result for the differential cross section:

$$\sigma(d\Omega\leftarrow\mathbf{k}_0) = d\Omega\frac{1}{k_{0z}\,k_0}\,|g(\mathbf{q}\leftarrow\mathbf{q}_0)|^2 \tag{22}$$

where from eq.(12):

$$g(\mathbf{q} \leftarrow \mathbf{q}_0) = \frac{4\pi}{A} \int d\mathbf{R}\, \sin\left(\eta(\mathbf{R})\right)\, e^{i\eta(\mathbf{R})}\, e^{i(\mathbf{q}_0 - \mathbf{q})\cdot\mathbf{R}} \tag{23}$$

What we are after is the total cross section for scattering by a defect. We next employ the differential cross section result to express this in terms of an optical theorem for surface scattering. To do so, we use the manifest unitarity of the SA expression, eq.(7). Separating once again the specular and non-specular parts of the S-matrix, now in operator form: $S = 1 + R$, and applying the unitarity condition, we have: $R + R^\dagger = -R\,R^\dagger$. Inserting a complete set and taking matrix elements:

$$\langle \mathbf{p}'|R|\mathbf{p}\rangle + \langle \mathbf{p}|R|\mathbf{p}'\rangle^* = -\int d^3p'' \langle \mathbf{p}''|R|\mathbf{p}'\rangle^* \langle \mathbf{p}''|R|\mathbf{p}\rangle \tag{24}$$

But it is clear from eq.(11) that:

$$\langle \mathbf{p}'|R|\mathbf{p}\rangle = \frac{i}{2\pi\, m\, p} g(\mathbf{q} \leftarrow \mathbf{q}')\, \delta(E_p - E_{p'})$$

Inserting this into eq.(24) and factoring out a common δ:

$$\frac{1}{p}\left(g(\mathbf{q}' \leftarrow \mathbf{q}) - g(\mathbf{q} \leftarrow \mathbf{q}')^*\right) = \frac{i}{2\pi\, m} \int d^3p''\, \delta(E_p - E_{p''})\, g(\mathbf{q}'' \leftarrow \mathbf{q}')^*\, g(\mathbf{q}'' \leftarrow \mathbf{q}) \frac{1}{(p'')^2} \tag{25}$$

The optical theorem results by considering the specular scattering ($\mathbf{q} = \mathbf{q}'$) and integrating over $\mathbf{p}''$. In contrast to two-body scattering, in the atom-surface scattering case only the space above the surface is available, which can be taken care of by a factor of $\frac{1}{2}$. Then, using $\int_0^\infty dp'\, h(p')\, \delta(E_p - E_{p'}) = \frac{m}{p} h(p)$ and performing the radial integration:

$$\begin{aligned}\int d^3p'' \cdots = \frac{1}{2} \int d\Omega_{\mathbf{p}''} \int_0^\infty p''^2\, dp''\, \delta(E_p - E_{p''})\, g^*(\mathbf{q}'' \leftarrow \mathbf{q}')\, g(\mathbf{q}'' \leftarrow \mathbf{q}) \frac{1}{p''^2} \\ = \frac{m}{2\,p} \int d\Omega_{\mathbf{p}''}\, g^*(\mathbf{q}'' \leftarrow \mathbf{q}')\, g(\mathbf{q}'' \leftarrow \mathbf{q})\end{aligned}$$

Using this and the specularity condition in eq.(25), we obtain:

$$\frac{2i}{p} \mathrm{Im}\left[g(\mathbf{q} \leftarrow \mathbf{q})\right] = \frac{i}{2\pi} \frac{1}{2p} \int d\Omega_{\mathbf{p}'}\, |g(\mathbf{q}' \leftarrow \mathbf{q})|^2 \tag{26}$$

Comparing the RHS of eq.(26) with that of eq.(22), we observe that it is just the *total* cross section for scattering at incidence momentum $\mathbf{p}$, i.e.:

$$\Sigma(\mathbf{p}) \equiv \int d\Omega_{\mathbf{p}'}\, \sigma(d\Omega_{\mathbf{p}'} \leftarrow \mathbf{p}) = \frac{1}{k\, k_z} \int d\Omega_{\mathbf{p}'}\, |g(\mathbf{q}' \leftarrow \mathbf{q})|^2$$

whence finally, the Optical Theorem:

$$\Sigma(\mathbf{k}) = \frac{8\pi}{k\, k_z} \mathrm{Im}\left[g(\mathbf{q} \leftarrow \mathbf{q})\right] \tag{27}$$

From eq.(23) we obtain an explicit form for the total cross section:

$$\Sigma(\mathbf{k}) = \frac{32\pi^2}{A\, k\, k_z} \int_{\mathrm{surf}} d\mathbf{R}\, \sin^2 \eta(\mathbf{R}) \tag{28}$$

Equation (28) is the optical theorem for surface scattering within the SA. As a final remark, we did not consider the effect of Bragg scattering from a periodical underlying surface. As shown by Xu *et al.*, [10] this contribution should be counted along with the specular amplitude, and its incorporation in the present framework should pose no particular difficulty.

IV. APPLICATIONS

We now illustrate a number of applications of our result.

A. Solvable Model of a Single Adsorbate

It has been known for long that the long-range attractive interaction is dominant in determining the He-adsorbate cross section. [24,11,6,9] We wish to identify the contribution of the short-range repulsive forces to the cross section. For this purpose, we will completely ignore the long-range attractive forces and consider a hard wall He-adsorbate interaction, where the adsorbate is described by a shape function $\xi(R)$. Then the potential takes the form:

$$V(\mathbf{r}) = \begin{cases} 0 & : z \geq \xi(\mathbf{R}) \\ \infty & : z < \xi(\mathbf{R}) \end{cases}$$

From the expression for the phase-shift eq.(8), it is clear that in this case:

$$\eta(\mathbf{R}) = -k_z\, \xi(\mathbf{R}) \tag{29}$$

We now consider a fully solvable model of a single adsorbate, which although highly artificial, will provide us with valuable insight regarding the role of the repulsive interaction in determining the general nature of the cross section. Let us assume a cylindrically symmetric shape function of the form:

$$\xi(\mathbf{R}) = h\,\zeta\left(|\mathbf{R}|/l\right) \qquad \zeta(\alpha) = \begin{cases} 0 & : \alpha > 1 \\ 1-\alpha^n & : 0 \le \alpha \le 1 \end{cases} \tag{30}$$

where h is the height of the adsorbate above the surface (effectively the strength of the coupling between the He and the adsorbate). $l = \gamma\, L$ $(0 \le \gamma \le 1)$ is a characteristic range of the He-adsorbate interaction. The unit-cell area (see section IIIIII A) is taken as $A = \pi L^2$. The linear extent of the entire surface is denoted R_s. We will demonstrate this choice of $\zeta(\alpha)$ to be analytically solvable in terms of known functions for $n = 1, 2, 4$. For $n = 1$ one obtains a cone, for $n = 2, 4$ the shape is a *convexly* deformed cone. It has a physically unreasonable sharp edge for $\alpha = 1$, yet the cases $n = 2, 4$ should be a crude, but reasonable model of the main features of the adsorbate shape function. In order to check the influence of the sharp edge, we may consider instead of ζ a *concave* shape function, which trades the edge with a sharp tip at $\alpha = 0$:

$$\xi(\mathbf{R}) = h\,\kappa\left(|\mathbf{R}|/l\right) \qquad \kappa(\alpha) = \begin{cases} 0 & : \alpha > 1 \\ (1-\alpha)^n & : 0 \le \alpha \le 1 \end{cases} \tag{31}$$

This model is solvable for $n = 1, 2$.

Using the symmetry, we have from the expression for the cross section within the SA (eq.(28)), for the convex case:

$$\Sigma(\mathbf{k}) = \frac{64\pi^2\,\gamma^2}{k\,k_z} \int_0^{\epsilon} d\alpha\; \alpha\; \sin^2\left[h\,k_z\,\zeta(\alpha)\right] \tag{32}$$

where $\epsilon \equiv R_s/l$. Defining $\beta \equiv h\,k_z$, and letting $I_n^{\zeta}(\beta)$, $I_n^{\kappa}(\beta)$ stand for the integrals (without the prefactors) in the convex and concave cases respectively, they evaluate to:

$$I_1^{\zeta}(\beta) = I_1^{\kappa}(\beta) = \frac{\epsilon^2}{4} + \frac{\cos(2\beta) - \cos(2\beta(1-\epsilon))}{8\,\beta^2} + \frac{\epsilon\sin(2\beta(1-\epsilon))}{4\,\beta}$$

$$I_2^{\zeta}(\beta) = \frac{\epsilon^2}{4} - \frac{\sin(2\beta) - \sin(2\beta(1-\epsilon^2))}{8\,\beta}$$

$$I_2^{\kappa}(\beta) = \frac{\epsilon^2}{4} + \frac{1}{4}\sqrt{\frac{\pi}{\beta}}\left[F_c\left(-2\sqrt{\beta/\pi}\right) - F_c\left(2\sqrt{\beta/\pi}(\epsilon-1)\right)\right] + \frac{\sin(2\,\beta) - \sin(2\,\beta(\epsilon-1)^2)}{8\,\beta}$$

$$I_4^{\zeta}(\beta) = \frac{\epsilon^2}{4} - \frac{1}{8}\sqrt{\frac{\pi}{\beta}}\left(\cos(2\beta)\,F_c\left(2\epsilon^2\sqrt{\beta/\pi}\right) + \sin(2\beta)\,F_s\left(2\epsilon^2\sqrt{\beta/\pi}\right)\right) \quad (33)$$

where F_c, F_s are the Fresnel integrals:

$$F_c(x) = \int_0^x \cos\left(\frac{\pi\,y^2}{2}\right)\,dy \qquad F_s(x) = \int_0^x \sin\left(\frac{\pi\,y^2}{2}\right)\,dy$$

An analysis of the models in the simple case of $\epsilon = 1$ yields the following results (see figure 1 - cone, figures 2, 3 - convex cases, figure 4 - concave cases):

- In both the concave and convex cases the cross section generally decreases with increasing incidence wave-number k_z.
- The convex model exhibits more noticeable oscillations. These are due to interference between He particles striking the top of the adsorbate and the surface. Since the top has a larger surface area in the convex case, the increased oscillations are expected.
- The cross section is generally larger in the convex case. This is also expected due to the larger surface area of the top.
- The cross section has a finite limit for $k_z \to 0$, which can easily be found by a first-order Taylor expansion of the $\sin^2$ in eq.(32). This limit is as a matter of fact beyond the region of validity of the SA. However, relying on the impressive success of the SA under unfavorable conditions of significant corrugation, [29] we consider the limit anyway: its dependence on the corrugation parameter h and the concavity/convexity parameter n is of high interest. We find:

$$\Sigma^{\zeta}(k \to 0) = \frac{32\pi^2\,h^2\,n^2}{(1+n)\,(2+n)} \qquad \text{(convex)}$$

$$\Sigma^{\kappa}(k \to 0) = \frac{32\pi^2\,h^2}{(1+n)\,(1+2\,n)} \qquad \text{(concave)}$$

The corrugation parameter h is thus seen to be of major importance in determining the cross section, which in the limit of low incidence energy scales as its square. The dependence on the exponent n is, as expected, opposite in the concave *vs.* convex case (see figure 5): in the former, the cross section monotonically decreases with n, whereas it increases in the latter. This is once again due to size of the surface area of the adsorbate top in each case.

- Due to the absence of the attractive part in our model, the resulting cross section values are too small. Typical values for e.g. CO/Pt(111) [2,3] are in the range $100 - 300\mathring{A}^2$. This deficiency of the hard wall model was already observed by Jonsson *et al.* [24,7]

- The integrals $I_n^\zeta(\beta)$, $I_n^\kappa(\beta)$ tend asymptotically to a constant value with k_z. Therefore the decrease in the cross section is entirely (apart from oscillations) due to the k_z^{-2} factor.

In conclusion, it appears that the cross sections we obtained exhibit all the general features of the experimentally observed ones: the oscillations, the decrease with increasing incidence energy and the finite limit for vanishing incidence energy. We conclude that while the long-range attractive part is important in the setting the *magnitude* of the cross section values (the stronger the interaction, the larger the cross section), at least for the high-energy regime the energy dependent features are already determined by the short-range repulsive interaction. In the next section we will significantly simplify the relation eq.(32) between the cross section and the shape function, without any further approximations, in order to be able to eventually invert the shape function from cross section measurements.

B. Inversion of Shape Function from Measurement of Cross Section

In this section we will demonstrate how the optical theorem result may be used to approximately solve the inversion problem for the He-adsorbate potential. The SA was already employed by Gerber, Yinnon and coworkers [31,32] for an approximate inversion of

the potential, by using the full angular intensity distribution. Here we will demonstrate a less general result for the inversion of the adsorbate shape function, which will, however, have the advantage of relying on a simpler measurement, of the specular intensities alone. We consider the case of a cylindrically symmetric adsorbate. If our unit-cell and the surface are circles of radii L and R_s respectively, then from eq.(28) we have for the adsorbate cross section:

$$\Sigma(k_z,\theta_{in}) = \frac{32\pi^2}{\pi L^2\, k_z^2 \cos(\theta_{in})} 2\pi \int_0^{R_s} \sin^2\eta(R)\, R\, dR = \frac{1}{\alpha\, k_z^2}\left[\frac{1}{2}R_s^2 \,-\, \int_0^{R_s} \cos\left(2\eta(R)\right) R\, dR\right] \tag{34}$$

where

$$\alpha \equiv \frac{L^2\, \cos(\theta_{in})}{32\pi^2}$$

(We note in passing that the often discussed [7] $\cos(\theta_{in})$ factor, θ_{in} being the angle between the incident direction and the surface normal, arises naturally in our formalism). Our demonstration in section II that this cross section is equivalent to that measurable by a specular attenuation experiment, ensures that the last equation can be regarded as a simple integral equation for the phase-shift η in terms of measurable quantities R_s, L and $\Sigma(k_z,\theta_{in})$. The measurable part is:

$$M(k_z) \equiv \frac{1}{2}{R_s}^2 \,-\, \alpha\, k_z^2\, \Sigma(k_z,\theta_{in}) \tag{35}$$

Let us now make the hard wall assumption again, which leads to the form of eq.(29) for the phase-shift. By doing so, we will be able to obtain the form of the shape function $\xi(\mathbf{R})$ of the adsorbate. Of course the concept of a shape function is rather artificial, yet it is of great interest in characterizing surface roughness, and is not unrelated to what is obtained in STM measurements. Defining for convenience:

$$\Theta(R) = 2\,\xi(R), \tag{36}$$

we can express the integral part as:

$$I_\Theta \equiv \int_0^{R_s} R\, dR \cos\left(k_z \Theta(R)\right) \tag{37}$$

so that eq.(34) becomes:

$$I_\Theta = M(k_z) \tag{38}$$

We next assume $\Theta(R)$ to be a monotone, single-valued function, so that we can consider its inverse $R(\Theta)$ (see figure 6). Thus:

$$I_\Theta = \int_{\Theta(0)}^{\Theta(R_s)} d\Theta\, \frac{dR(\Theta)}{d\Theta} R(\Theta)\, \cos(k_z \Theta) = \frac{1}{\sqrt{2\pi}} \int_{\Theta(0)}^{\Theta(R_s)} d\Theta\, F(\Theta)\, \left(e^{i\, k_z\, \Theta} + e^{-i\, k_z\, \Theta}\right) \tag{39}$$

where we defined:

$$F(\Theta) = \frac{\sqrt{2\pi}}{4} \frac{d\left(R^2(\Theta)\right)}{d\Theta} \tag{40}$$

$R(\Theta)$ is confined, so it is convenient to define a "box" function:

$$b(\Theta) = \begin{cases} 1 \ : \ \Theta(R_s) \leq \Theta \leq \Theta(0) \\ 0 \ : \ \text{else} \end{cases} \tag{41}$$

which allows us to write I_Θ as a Fourier transform of a product:

$$I_\Theta = \mathcal{F}\left[F(\Theta)\, b(\Theta);\ k_z\right] \ + \ \mathcal{F}^{-1}\left[F(\Theta)\, b(\Theta);\ k_z\right] \tag{42}$$

where we introduced a notation for the Fourier transform,

$$\mathcal{F}\left[f(x);\ y\right] = \frac{1}{\sqrt{2\pi}} \int_{-\infty}^{\infty} dx\, f(x)\, e^{i\, x\, y}$$

To isolate $F(\Theta)$ we apply an inverse Fourier transform to eq.(42), yielding:

$$F(\Theta)\, b(\Theta) \ + \ F(-\Theta)\, b(-\Theta) = \mathcal{F}^{-1}\left[I_\Theta(k_z);\ \Theta\right] \tag{43}$$

But $\Theta > 0$ so that by definition of the box function the second term in eq.(43) vanishes, and we obtain from it, upon inserting the definitions of M (eq.(35)) and F (eq.(40)):

$$\frac{\sqrt{2\pi}}{4} \frac{d\left(R^2(\Theta)\right)}{d\Theta} = \pi\, {R_s}^2\, \delta(\Theta) \ - \ \alpha\, \mathcal{F}^{-1}\left[k_z^2\, \Sigma(k_z, \theta_{in});\ \Theta\right] \qquad \text{for} \ \ \Theta(R_s) \leq \Theta \leq \Theta(0) \tag{44}$$

If we assume that the shape function never fully vanishes ($\Theta(R_s) > 0$) then $\delta(\Theta) = 0$, so that finally:

$$\frac{d\left(R^2(\Theta)\right)}{d\Theta} = -\frac{L^2\,\cos(\theta_{in})}{8\pi^2\sqrt{2\pi}}\mathcal{F}^{-1}\left[k_z^2\,\Sigma_{\theta_{in}}(k_z);\;\Theta\right] \tag{45}$$

The last equation is the sought after inversion. Its RHS should be considered as calculated from the experimental data on the cross section as a function of the incidence wavenumber, at a given incidence angle. The inversion is completed by solving for $R^2(\Theta)$ under the condition $R(0) \to \infty$, and retrieving the shape function $\xi(R) = \frac{1}{2}\Theta(R)$.

In practice, however, it is more reasonable to assume a functional form for $\Theta(R)$ with free parameters, to be fitted based on the experimental data. The somewhat artificial concept of a shape function may not justify an attempt to determine an actual *function* from the cross section data, as implied by eq.(45). This could be problematic due to the discreteness and finiteness of the available data set. If we assume this approach, a further simplification can be obtained by returning to eq.(39) and integrating by parts (with $\Theta(R_s) = 0$ - an excellent approximation):

$$I_\Theta = \frac{1}{2}\left[R_s^2 - k_z\int_0^{\Theta(0)} d\Theta\; R^2(\Theta)\,\sin\left(k_z\,\Theta\right)\right] \tag{46}$$

Equating this according to eq.(38) to $M(k_z)$, and assuming that we have guessed a functional form for $\Theta(R)$ with a set of free parameters $\{\alpha_i\}$, the inversion result may now be stated in the form:

$$\frac{\cos(\theta_{in})}{(4\pi)^2}\Sigma_{\theta_{in}}(k_z) = g\left(k_z;\{\alpha_i\}\right) \qquad g\left(k_z;\{\alpha_i\}\right) \equiv \frac{1}{L^2\,k_z}\int_0^{\Theta(0)} d\Theta\; R^2(\Theta;\{\alpha_i\})\,\sin\left(k_z\,\Theta\right) \tag{47}$$

The remaining task is to find the set $\{\alpha_i\}$ which gives the best fit for the chosen form of g to the cross section data. In the next section we shall implement this approach on experimental data. Alternatively, the last result may be viewed as a theoretical expression for the cross section, within the SA and a hard wall model.

C. Fit of Shape Function for Ag on Pt(111)

We now employ our inversion result to obtain a fit for a shape function of an Ag atom on a Pt(111) surface, based on He scattering measurements by P. Zeppenfeld. [25] The shape function is a legitimate and highly relevant object of study in the field of surface roughness. It basically corresponds to an equipotential surface, and therefore within a certain approximation, [33,34] also to the core electron densities. As a result, it is a complementary quantity to what is measured in STM experiments, where one probes the electron densities at the Fermi level. Assuming cylindrical symmetry, the shape function should have the general form depicted in figure 6: it should be flat and smooth at its top, and decay to zero height far away from the nucleus. This leads us to consider two simple forms for the shape function: a Lorentzian and a Gaussian, with two free parameters l, Θ_0 each. Thus:

$$\Theta_L(R) = \frac{\Theta_0}{1 + \left(\frac{R}{l}\right)^2} \quad \text{or} \quad \Theta_G(R) = \Theta_0\, e^{-\left(\frac{R}{l}\right)^2} \tag{48}$$

Inverting these for $R^2(\Theta)$ leads to integrals $g\left(k_z; \{\alpha_i\}\right)$ (eq.(47)) expressible in terms of known functions:

$$g_L\left(k_z; \{l, \Theta_0\}\right) = \frac{l^2}{L^2}\left(\frac{(\cos(k_z\,\Theta_0) - 1)}{k_z^2} + \frac{\Theta_0\,\mathrm{si}(k_z\,\Theta_0)}{k_z}\right) \tag{49}$$

$$g_G\left(k_z; \{l, \Theta_0\}\right) = \frac{l^2}{L^2}\frac{1}{k_z^2}\left(\Gamma + \ln(k_z\,\Theta_0) - \mathrm{ci}(k_z\,\Theta_0)\right) \tag{50}$$

where $\mathrm{si(x)}, \mathrm{ci(x)}$ are the sine and cosine integrals respectively, and Γ is Euler's constant (0.5772..). Both g_L and g_G contain an oscillatory part, expressing the interference between parts of the He beam striking the top of the adsorbate and the flat surface, and both decay as k_z^{-2} for large k_z. The parameters l (the He-adsorbate interaction range) and L (the unit-cell extent) appear only in the combination l^2/L^2, and may hence be treated as a single dimensionless parameter $\gamma \equiv l/L$. This result is easily seen to hold for any shape function of the form $\Theta\left(R/l\right)$, as was already demonstrated in section IVIV A The dependence of the cross section on the He-adsorbate interaction range thus contains no surprises: the cross

section scales as the square of this range. It is the adsorbate height Θ_0, i.e., the coupling coefficient between the He and the adsorbate, which plays the interesting role. It determines the frequency of oscillations of the cross section, and affects its magnitude.

Using the results for the Lorentzian and Gaussian models, eqs.(49,50) respectively, in the expression for the cross section, eq.(47) we calculated best-fits for the parameters Θ_0 and γ. The fits are shown along with the empirical cross section values [25] in figure 7. The deviations are 1.47% for the Lorentzian, 1.14% for the Gaussian. The fits do not follow the oscillations in the data closely, but these are uncertain anyway due to the large experimental error ($\sim 20\%$). The values found are:

Lorentzian: $\Theta_0 = 1.51\mathring{A}$, $\gamma = 0.93$

Gaussian: $\Theta_0 = 1.05\mathring{A}$, $\gamma = 1.83$

The values for the adsorbate "height" Θ_0 are in reasonable agreement with those obtained from STM measurements. [25] That $\gamma > 1$ for the Gaussian model expresses the fact that the He-adsorbate interaction range extends beyond the adsorbate unit-cell. In any inversion problem, the question of stability is major importance. In the present case, convergence to the fitted values is overall better for the Gaussian model, which also has a smaller deviation: the Gaussian model converges to the same values for initial guesses of $0 < \Theta_0 < 5\mathring{A}$, whereas convergence is obtained for the Lorentzian model only for the smaller range of $0 < \Theta_0 < 3\mathring{A}$. The initial value of the parameter γ has almost no influence on the convergence. When compared over a large range of k_z values (see figure 8), the two models are seen to essentially differ in their prediction of the cross section merely by a shift. The situation is different, however, when we compare the sought-after quantity: the shape function. The corresponding shape functions are shown in figure 9. The Lorentzian model is much more peaked and narrow. Intuitively, it seems that the Gaussian shape is better suited to describe the adatom shape function, in agreement with the relative deviations and convergences.

D. Inversion of Potential for Weakly Corrugated Surfaces

Consider a surface of substrate type A, in which one of the atoms is replaced by an atom of type B, such that the radii differ only slightly. This is an example of a surface with weak corrugation due to substitutional disorder. Let the surface be flat and located at $z = 0$. The interaction potential with an incident He atom may be written approximately as:

$$U(R, z) = U_s(z) + U_d(R^2 + z^2)\,, \qquad |U_s| \gg |U_d| \tag{51}$$

where $\mathbf{R} = (x, y)$, $V_s = \frac{\hbar^2}{2m} U_s$ is the contribution of the surface, and $V_d = \frac{\hbar^2}{2m} U_d$ is the interaction with the defect, assumed spherically symmetric. We next assume $V_s(z)$ is known and wish to determine V_d from the scattering data. We note that a similar inversion has already been considered by Gerber, Yinnon and coworkers, [31,32] but for defectless, crystalline surfaces. When the condition $|U_s| \gg |U_d|$ is used in eq.(8), a first order expansion yields:

$$\begin{aligned} \eta(R) &\approx \eta_0(R) + \frac{1}{2}\eta_1(R) \\ \eta_0(R) &= \int_{z_t(R)}^{\infty} dz \, \left[\left({k_z}^2 - U_s(z) \right)^{\frac{1}{2}} - k_z \right] - k_z \, z_t(\mathbf{R}) \\ \eta_1(R) &= -\int_{z_t(R)}^{\infty} dz \, \frac{U_d(R^2 + z^2)}{\left({k_z}^2 - U_s(z) \right)^{\frac{1}{2}}} \end{aligned} \tag{52}$$

The turning-point function $z_t(R)$ may either be measured by the inversion procedure described in section IVIV B for the shape function ξ, or approximated as the solution to $V_s(z) = E$, i.e., neglecting V_d altogether. In either case $\eta_0(R)$ is a known quantity. Let us next use our approximation for η in eq.(34). Then after a first order expansion about $2\eta_0$:

$$\alpha k_z^2 \, \Sigma(k_z, \theta_{in}) - \frac{1}{2} R_s^2 + \int_0^{R_s} dR \, R \, \cos(2\eta_0) \approx \int_0^{R_s} dR \, R \, \sin(2\eta_0(R)) \, \eta_1(R) \tag{53}$$

The LHS consists of measurable/known quantities and we denote it $M_1(k_z)$. The RHS contains the unknown function U_d which we are after; we denote it $I(k_z)$. Using the definition of η_1 (eq.(52)):

$$I(k_z) = -\int_0^{R_s} dR\, R\, \sin(2\eta_0(R)) \int_{z_t(R)}^{\infty} dz\, \frac{U_d(R^2+z^2)}{\left({k_z}^2 - U_s(z)\right)^{\frac{1}{2}}} \tag{54}$$

A practical approach at this point would be to expand $U_d(R^2+z^2)$ in some convenient basis $\{f_n(R^2+z^2)\}$: $U_d(R^2+z^2) = \sum c_n f_n(R^2+z^2)$, so that:

$$\sum c_n \int_0^{R_s} dR\, R\, \sin(2\eta_0(R)) \int_{z_t(R)}^{\infty} dz\, \frac{f_n(R^2+z^2)}{\left({k_z}^2 - U_s(z)\right)^{\frac{1}{2}}} = -M_1(k_z) \tag{55}$$

This linear system can then be solved for as many c_n as there are data points (in k_z). A convenient choice of (non-orthogonal) basis functions are Gaussians, since then the double integral decouples into a product (neglecting the R-dependence of z_t). This approach should give a reasonable approximation to the defect potential. Powerful methods to deal with related numerical inversion problems, employing functional sensitivity analysis, have been developed by Ho and Rabitz. [35,36]

However, with some further assumptions it is also possible to perform an actual inversion for U_d, by combining the technique of section IVIV B and an Abel transform. We proceed to show this.

Our first two additional assumptions are:

- The interaction with the surface is purely repulsive, so that $\zeta = U_s(z)$ is a monotonously decreasing function.
- Also $\rho = \eta_0(R)$ is a monotone function. That this is reasonable can be seen by considering a hard-wall system; then a monotonously decreasing shape function (see section IVIV B) induces a monotonously increasing phase shift, by eq.(29).

Under these assumptions we may consider the inverse functions $z(\zeta)$ and $R(\rho)$. The transformation to the variable ζ decouples the integration limits if we make the fair approximation that $k_z^2 = U_s(z_t(R))$ (i.e., neglecting U_d), for then:

$$\int_{z_t(R)}^{\infty} dz\, \frac{U_d(R^2+z^2)}{\left({k_z}^2 - U_s(z)\right)^{\frac{1}{2}}} = \int_{k_z^2}^{0} d\zeta\, \frac{dz}{d\zeta} \frac{U_d(R,\zeta)}{\left({k_z}^2 - \zeta\right)^{\frac{1}{2}}}$$

and hence:

$$I(k_z) = \int_{k_z^2}^{0} d\zeta \left({k_z}^2 - \zeta\right)^{-\frac{1}{2}} f(\zeta) \qquad \text{where}$$
$$f(\zeta) = \frac{dz}{d\zeta} \int_0^{R_s} dR\, R\, \sin(2\eta_0(R))\, U_d(R,\zeta) \tag{56}$$

The above expression has the form of the familiar Abel transform, for which an explicit inversion exists:

$$f(\zeta) = -\frac{1}{\pi} \int_0^{\zeta} dk_z^2\, \frac{dI(k_z)}{dk_z^2} \left(\zeta - k_z^2\right)^{-\frac{1}{2}} \tag{57}$$

We rewrite this, using $I = M_1$ (eq.(53)) and changing variables from R to ρ, as:

$$J \equiv -\int_{\rho(0)}^{\rho(R_s)} d\rho\, U_d(\rho,\zeta)\, \frac{dR}{d\rho}\, R(\rho)\, \sin(2\rho) = G(\zeta, k_z) \tag{58}$$

where:

$$G(\zeta, k_z) = \frac{1}{\pi} \frac{d\zeta}{dz} \int_0^{\zeta} dk_z^2\, \frac{dM_1(k_z)}{dk_z^2} \left(\zeta - k_z^2\right)^{-\frac{1}{2}} \tag{59}$$

The function $G(\zeta, k_z)$ consists entirely of known quantities. We are still left with the task of isolating the potential U_d. But it is clear that J in eq.(58) is almost identical to I_Θ in eq.(39). In order to be able to use the Fourier transform technique applied to I_Θ, we must now introduce one additional assumption:

- $\eta_0(R)$ may reasonably well be approximated in the "hard-wall" form: $\eta_0(R) = -k_z \xi(R)$. Here $\xi(R)$ is to be considered known from the inversion of cross section data as described in section IVIV B Hamburger *et al.* [22] have shown that this form holds quite well also for realistic potentials.

Changing variables to $\Theta = 2\xi(R)$:

$$J = \int_{\Theta(0)}^{\Theta(R_s)} d\Theta \left[U_d(\Theta,\zeta) \frac{dR}{d\Theta} R(\Theta)\right] \sin(k_z \Theta)$$
$$= \frac{1}{\sqrt{2\pi}} \int_{\Theta(0)}^{\Theta(R_s)} d\Theta\, F(\Theta) \left(e^{ik_z\Theta} - e^{-ik_z\Theta}\right) \equiv I_\Theta \tag{60}$$

where now:

$$F(\Theta) = \frac{\sqrt{2\pi}}{4i} \frac{d(R^2(\Theta))}{d\Theta} U_d(\Theta, \zeta) \tag{61}$$

Repeating the arguments leading to eq.(45) and remembering that now $I_\theta = G(\zeta, k_z)$, we finally obtain:

$$U_d(\Theta, \zeta) = \frac{1}{\frac{d(R^2(\Theta))}{d\Theta}} \frac{4i}{\sqrt{2\pi}} \mathcal{F}^{-1} \left[G(\zeta, k_z); \Theta \right] \tag{62}$$

Formally, this completes the inversion.

V. CONCLUDING REMARKS

In this paper we investigated theoretically the cross section of a defect on a surface. We found that this quantity, when available from experiments, contains important information on the defect and its interaction with an incoming atom. We demonstrated that the cross section can be used for such purposes as an inversion to yield the shape function of a defect, an approximate inversion to give the interaction potential with a substituted atom, and evaluation of the role of the long-range repulsive forces in the interaction with an incident atom. The single most important advantage of the cross section is probably that it is so easily measurable, by employing the definition of the cross section proposed by Poelsema and Comsa. [1] This operational definition was shown here to be equivalent to the standard formal definition of quantum scattering theory, and hence either can be used interchangeably. Using the formal definition and the Sudden approximation, [23] we derived a form of the Optical theorem which is quite amenable to analytical study. Future work may benefit from this expression for the cross section. For example, it seems that extracting various probability distributions characterizing dilute surface disorder (such as a distribution of radii for hemispherical defects) should prove possible within this framework. Traditional approaches tended to rely on differential cross section measurements for inversion applications. Our general message for future work is that the total cross section, which is much easier to obtain experimentally, will be a highly fruitful subject of study for the purpose of both structural and dynamical characterization of isolated defects. Indeed,

a very promising possibility for future work should be one of measuring cross sections for surface defects of interest, and using this data in a corresponding theoretical effort to extract information on the position of the defect, its geometric shape, and its interaction potential with the incident atom. The latter is especially important, since the interaction potential contains information on the electronic density structure of the defect. We emphasize that cross sections measurements, when performed over a wide range of energies and incidence angles, may well become a new type of surface microscopy. We are currently pursuing efforts along this line, in cooperation with the experiments of P. Zeppenfeld.

ACKNOWLEDGMENTS

This research was supported by the German-Israeli Foundation for Scientific Research (G.I.F.), under grant number I-215-006.5/91 (to R.B.G.). Part of this work was carried out with support from the Institute of Surface and Interface Science (ISIS) at UC Irvine. The Fritz Haber Center at the Hebrew University is supported by the Minerva Gesellschaft für die Forschung, Munich, Germany. We are very grateful to Drs. P. Zeppenfeld and M. A. Krzyzowski for helpful discussions and allowing us to use their Ag/Pt(111) data prior to publication. We would also like to thank Dr. A.T. Yinnon for very useful discussions.

REFERENCES

[1] B. Poelsema, G. Comsa, Faraday Discuss. Chem. Soc., **80**, 16 (1985).

[2] B. Poelsema, S.T. deZwart, G. Comsa, Phys. Rev. Lett., **49**, 578 (1982).

[3] B. Poelsema, S.T. deZwart, G. Comsa, Phys. Rev. Lett., **51**, 522 (1983).

[4] B. Poelsema, L.K. Verheij, G. Comsa, Phys. Rev. Lett., **49**, 1731 (1982).

[5] B. Poelsema, R.L. Palmer, G. Comsa, Surf. Sci., **136**, 1 (1984).

[6] B.Poelsema and G. Comsa In Springer Tracts in Modern Physics, Vol. 115, *Scattering of Thermal Energy Atoms from Disordered Surfaces*, (Springer Verlag, Berlin, 1989).

[7] H. Jonsson, J. Weare, A.C. Levi, Surf. Sci., **148**, 126 (1984).

[8] W.-K. Liu, Faraday Discuss. Chem. Soc., **80**, 17 (1985).

[9] B. Gumhalter, D. Lovrić, Surf. Sci., **178**, 743 (1986).

[10] H. Xu, D. Huber, E.J. Heller, J. Chem. Phys., **89**, 2550 (1988).

[11] A.T. Yinnon, R. Kosloff, R.B. Gerber, B. Poelsema, G. Comsa, J. Chem. Phys., **88**, 3722 (1988).

[12] S.D. Bosanac, M.Sunic, Chem. Phys. Lett., **115**, 75 (1985).

[13] B. Gumhalter, W.-K. Liu, Surf. Sci., **148**, 371 (1984).

[14] G. Petrella, A.T. Yinnon, R.B. Gerber, Chem. Phys. Lett., **158**, 250 (1989).

[15] B. Poelsema, A.F. Becker, G. Rosenfeld, R. Kunkel, N. Nagel, L.K. Verheij, G. Comsa, Surf. Sci., **272**, 269 (1992).

[16] R. Kunkel, B. Poelsema, L.K. Verheij, G. Comsa, Phys. Rev. Lett., **65**, 733 (1990).

[17] Y.-W. Yang, H. Xu, T. Engel, J. Phys. Chem., **97**, 1749 (1993).

[18] H. Xu, Y.-W. Yang, T. Engel, Surf. Sci., **255**, 73 (1991).

[19] P. Dastoor, M. Arnott, E.M. McCash, W. Allison, Surf. Sci., **272**, 154 (1992).

[20] B.J. Hinch, C. Koziol, J.P. Toennies, G. Zhang, Europhys. Lett., **10**, 341 (1989).

[21] S.A. Safron, J. Duan, G.G. Bishop, E.S. Gillman, J.G. Skofronick, J. Phys. Chem., **97**, 1749 (1993).

[22] D.A. Hamburger, A.T. Yinnon, I. Farbman, A. Ben-Shaul, R.B. Gerber, submitted to Surf. Sci.

[23] R.B. Gerber, In Delgado-Bario, editor, *Dynamics of Molecular Processes*, page 299, IOP, (1993).

[24] H. Jonsson, J. Weare, A.C. Levi, Phys. Rev. B, **30**, 2241 (1984).

[25] P. Zeppenfeld, private communication.

[26] J.R. Taylor, *Scattering Theory: The Quantum Theory of Nonrelativistic Collisions*, (Robert E. Krieger Publishing Company, Florida, 1987).

[27] R.B Gerber, A.T. Yinnon, J.N. Murrel, Chem. Phys., **31**, 1 (1978).

[28] R.B. Gerber, Chem. Rev., **87**, 29 (1987).

[29] A.T. Yinnon, R.B. Gerber, D.K Dacol, H. Rabitz, J. Chem. Phys., **84**, 5955 (1986).

[30] D.A. Hamburger, R.B. Gerber, to be published.

[31] R.B. Gerber, A.T. Yinnon, J. Chem. Phys., **73**, 3232 (1980).

[32] A.T. Yinnon, E. Kolodney, A. Amirav, R.B. Gerber, Chem. Phys. Lett., **123**, 268 (1986).

[33] N. Esbjerg, J.K. Norskov, Phys. Rev. Lett., **45**, 807 (1980).

[34] N. D. Lang, J.K. Norskov, Phys. Rev. B, **27**, 4612 (1983).

[35] T.-S. Ho, H. Rabitz, J. Chem. Phys., **94**, 2305 (1991).

[36] T.-S. Ho, H. Rabitz, J. Chem. Phys., **96**, 7092 (1992).

FIGURES

FIG. 1. Cross section in the cone case ($n = 1$), for two values of the corrugation parameter h. The cross sections are almost identical, except for the behavior at small k_z.

FIG. 2. Cross section in the convex case ($n = 2$), for two values of the corrugation parameter h. The stronger the corrugation, the faster and more pronounced are the oscillations, and the larger the cross section for small k_z.

FIG. 3. Cross section in the convex case, for three values of the convexity parameter n, at a constant corrugation $h = 1\mathring{A}$. The higher the convexity, the faster and more pronounced are the oscillations, and the larger the cross section for small k_z.

FIG. 4. Cross section in the concave case for two values of the concavity parameter n, at a constant corrugation $h = 1\mathring{A}$. The larger the concavity, the smaller the cross section. Oscillations are virtually unnoticeable.

FIG. 5. Cross section for $k_z \to 0$, in the concave and convex cases, as a function of the concavity/convexity parameter. The more concave (i.e. peaked), the smaller the cross section. The opposite happens the more convex (i.e. rectangular) the shape function.

FIG. 6. General form of the shape function $\Theta(R)$ and its inverse $R(\Theta)$. The shape function should have a smooth top and monotonously decrease over a substantial range. We ignore the possibility of a subsequent increase.

FIG. 7. Cross section data for single Ag atom on Pt(111) (circles), along with fits for Lorentzian (solid line) and Gaussian (dashed line) shape function models. The agreement with the Gaussian model is somewhat better.

FIG. 8. Behavior of the cross sections of the Lorentzian and Gaussian models over a large range of incidence wave numbers. The two models predict a similar behavior, differing essentially by a shift along the y-axis.

FIG. 9. Shape functions of the Ag adatom for the Lorentzian and Gaussian models, using the parameters obtained by fitting the predicted cross sections to the measured one. The Gaussian model has a smoother top and is less narrowly peaked, in agreement with intuitive expectation for the "correct" shape. Note the different scales along the x and y-axes.

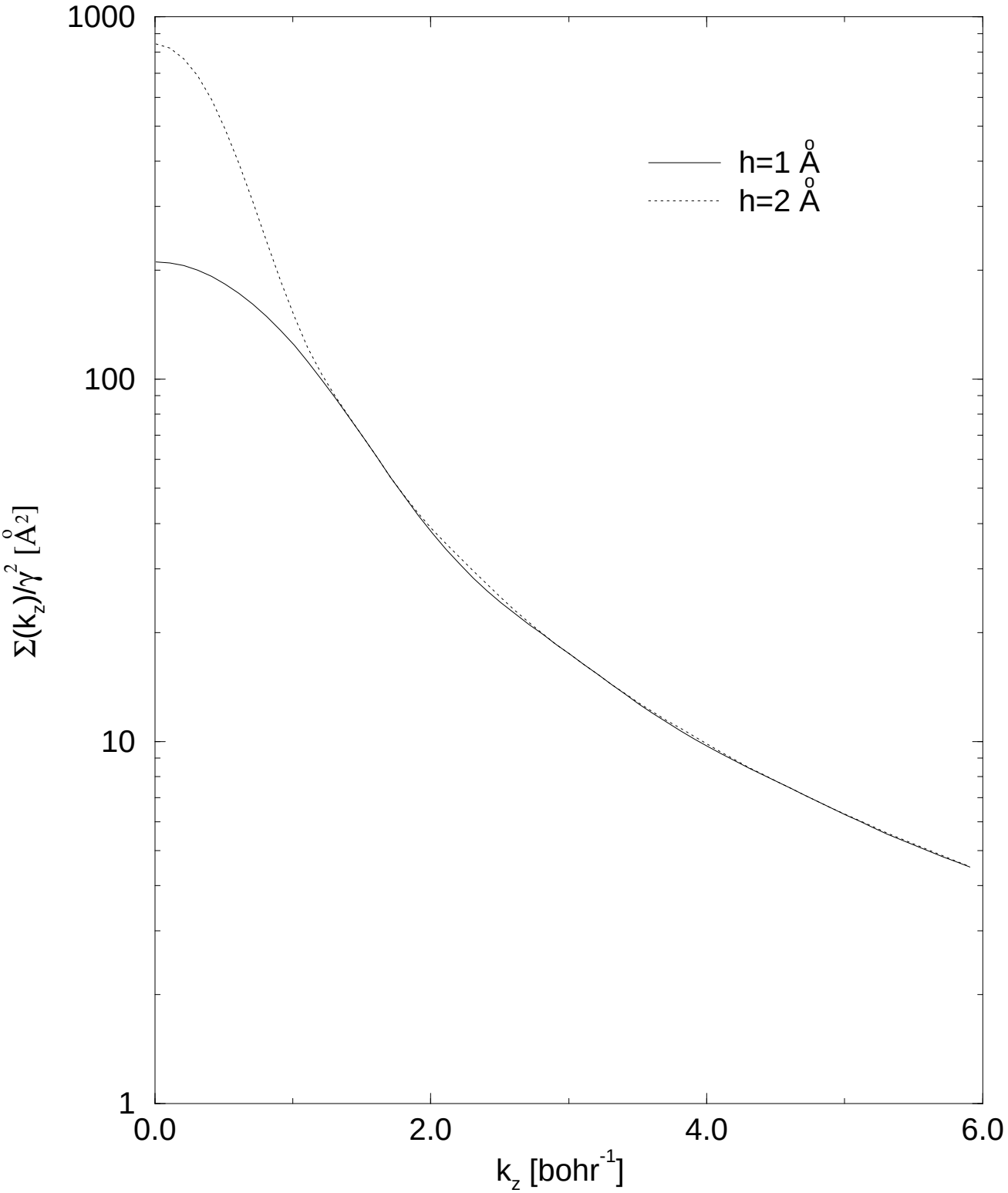
1000
100
10
1
0.0
2.0
4.0
6.0
h=1 Å
h=2 Å
$\Sigma(k_z)/\gamma^2$ [Å^2]
k_z [bohr^{-1}]

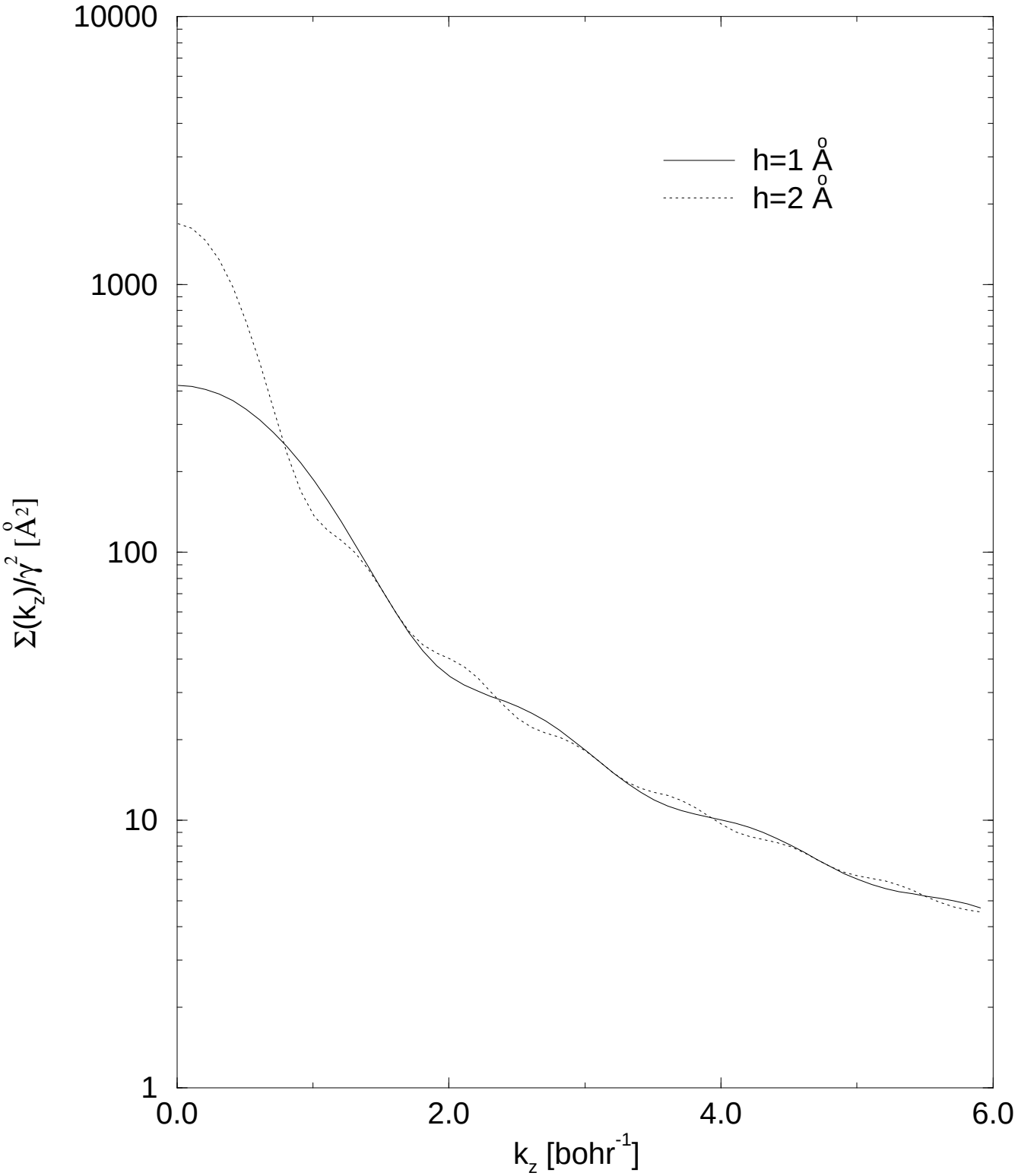
10000
1000
100
10
1
0.0
2.0
4.0
6.0
h=1 Å
h=2 Å
Σ(k_z)/γ^2 [Å^2]
k_z [bohr^-1]

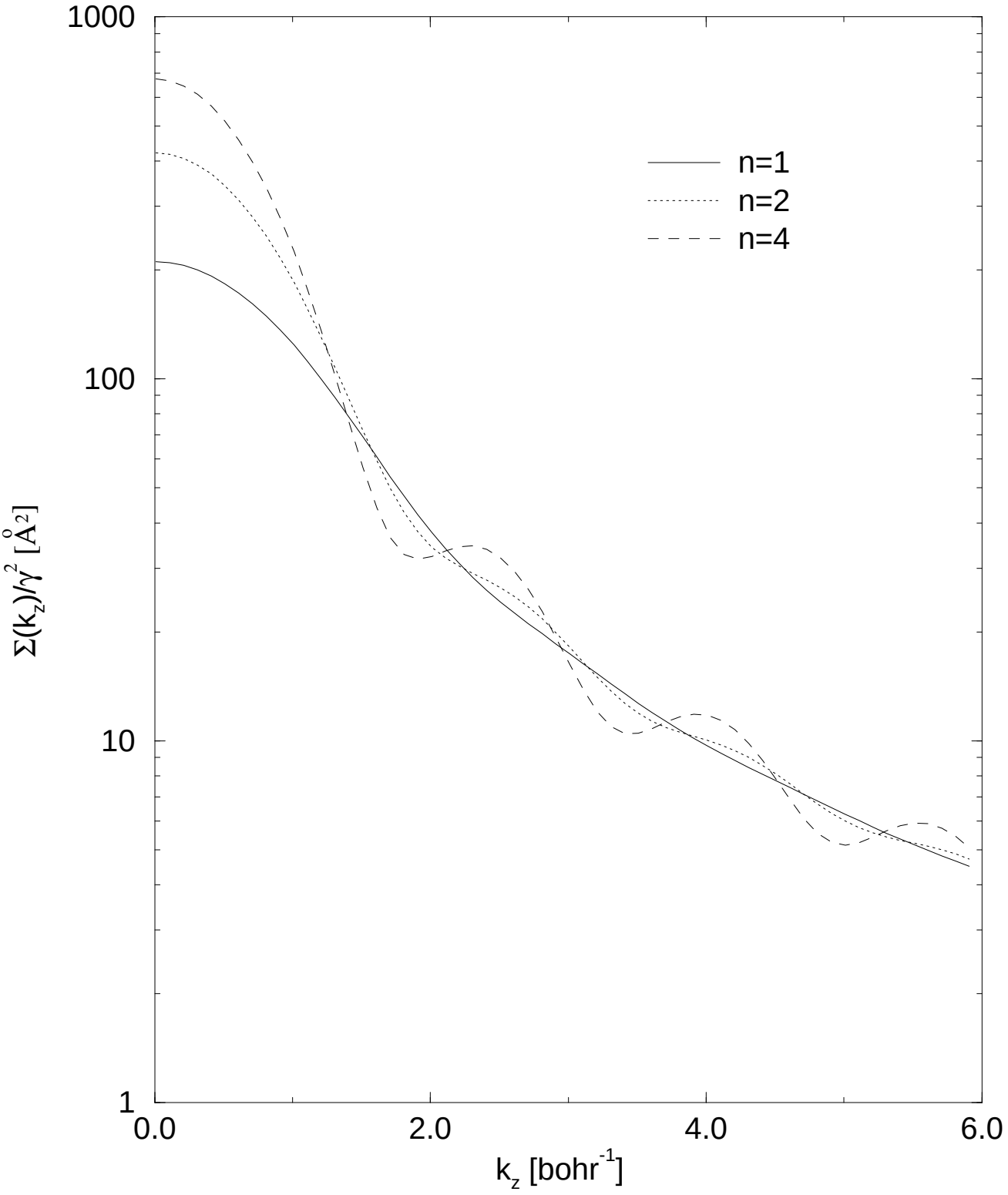
1000
100
10
1
0.0
2.0
4.0
6.0
n=1
n=2
n=4
$\Sigma(k_z)/\gamma^2$ [Å^2]
k_z [bohr^{-1}]

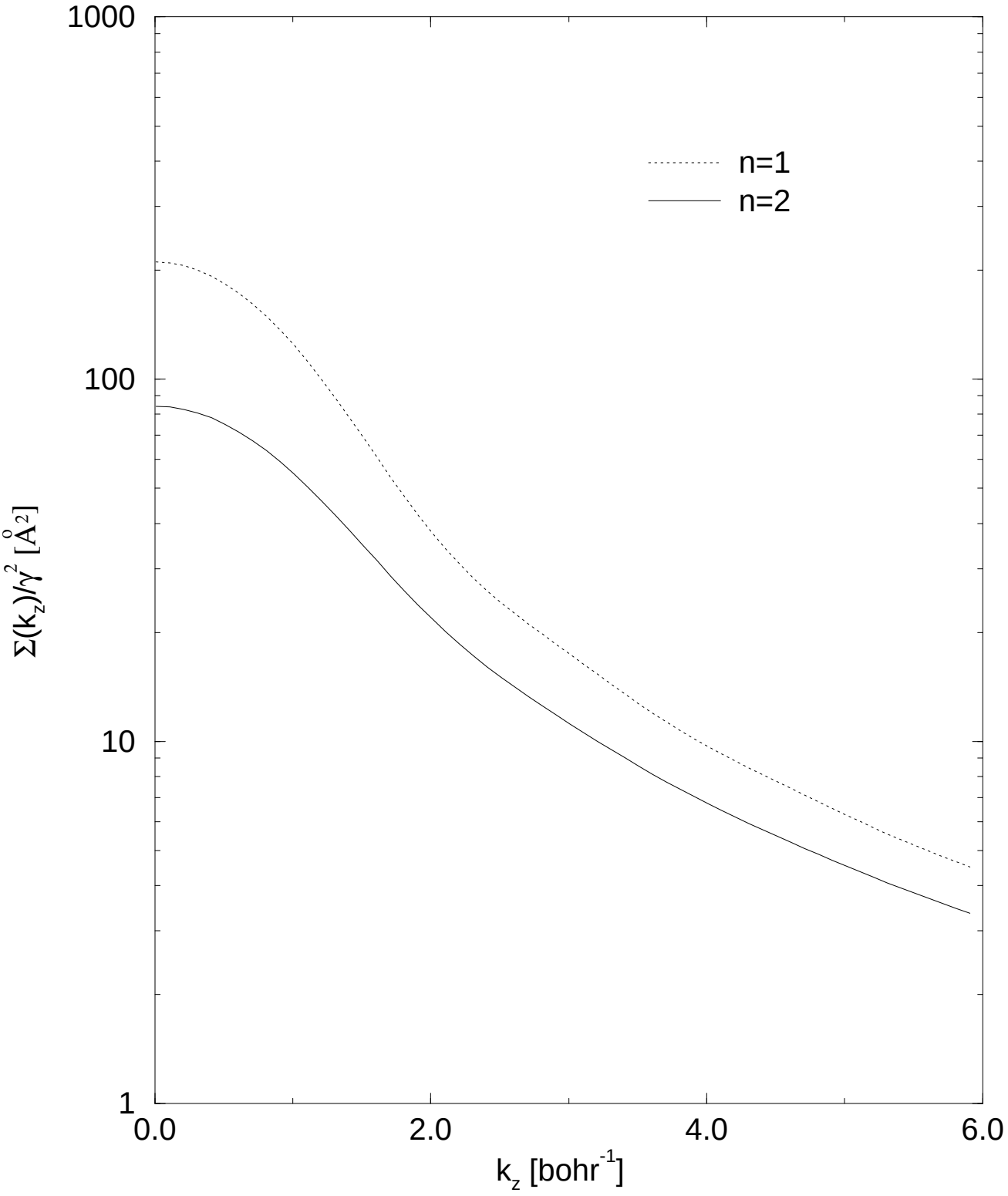
1000
100
10
1
0.0
2.0
4.0
6.0
n=1
n=2
$\Sigma(k_z)/\gamma^2$ [Å^2]
k_z [bohr^{-1}]

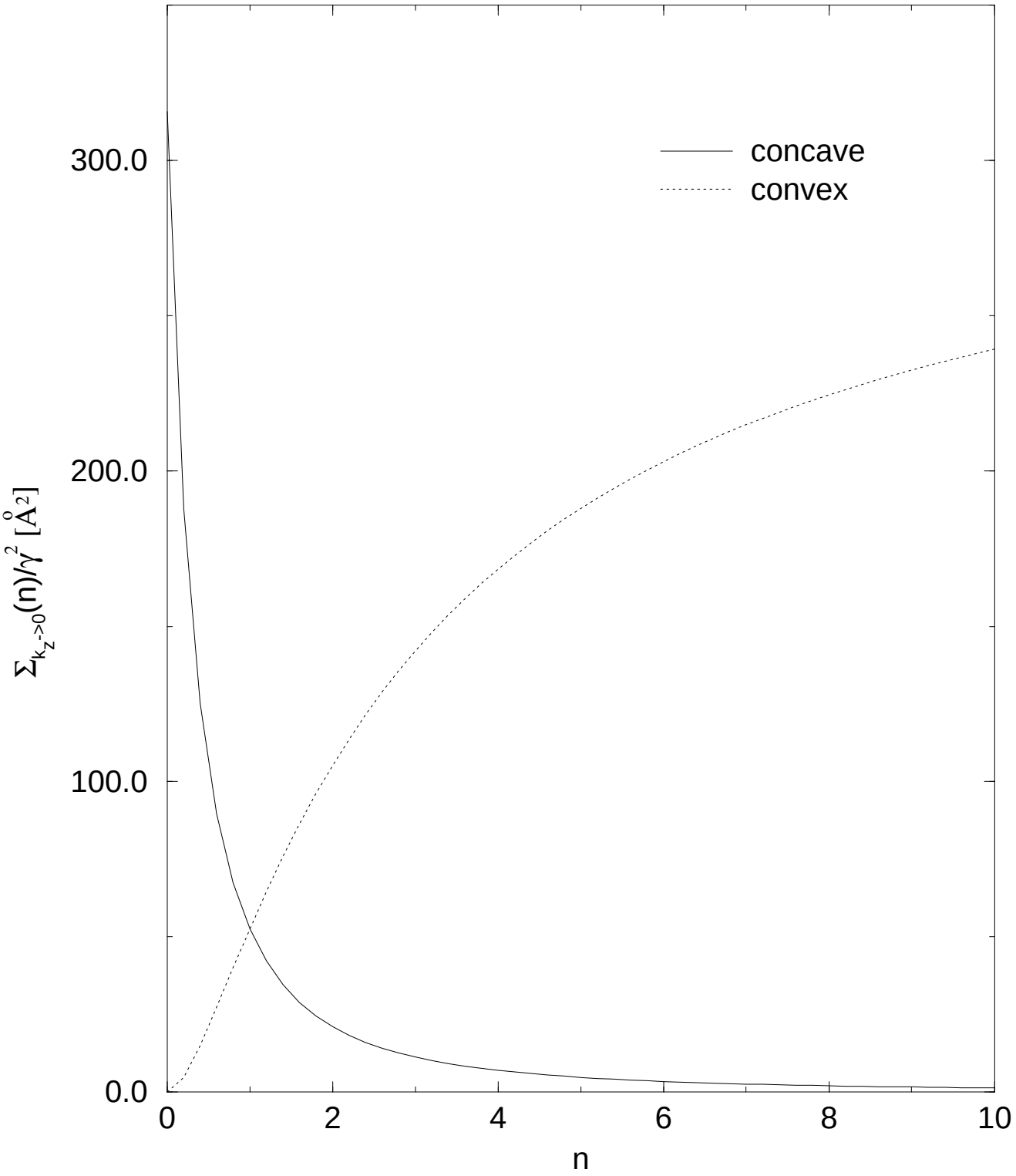
concave
convex
300.0
200.0
100.0
0.0
0
2
4
6
8
10
n
$\Sigma_{k_z->0}(n)/\gamma^2$ [Å^2]

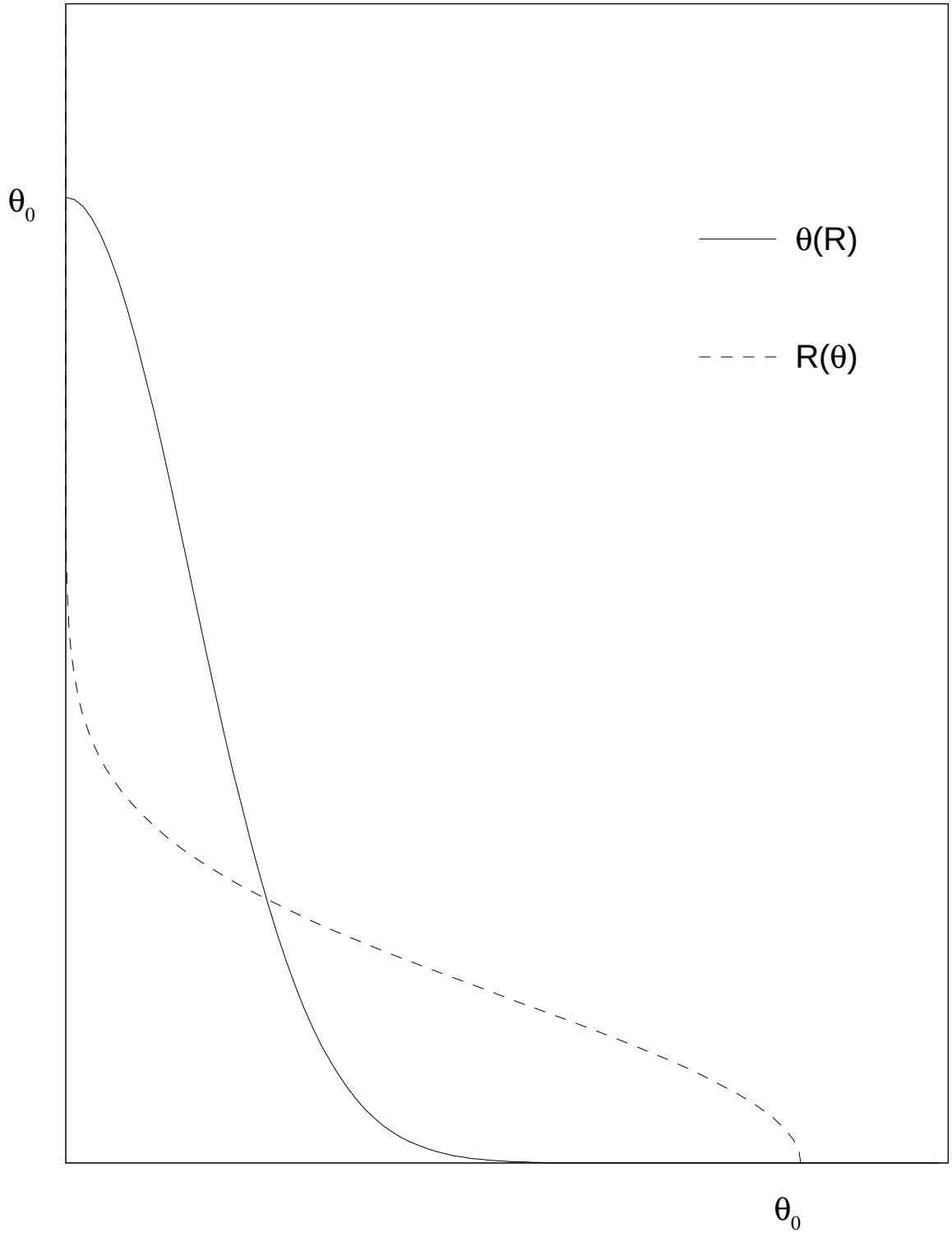
θ0
θ(R)
R(θ)
θ0

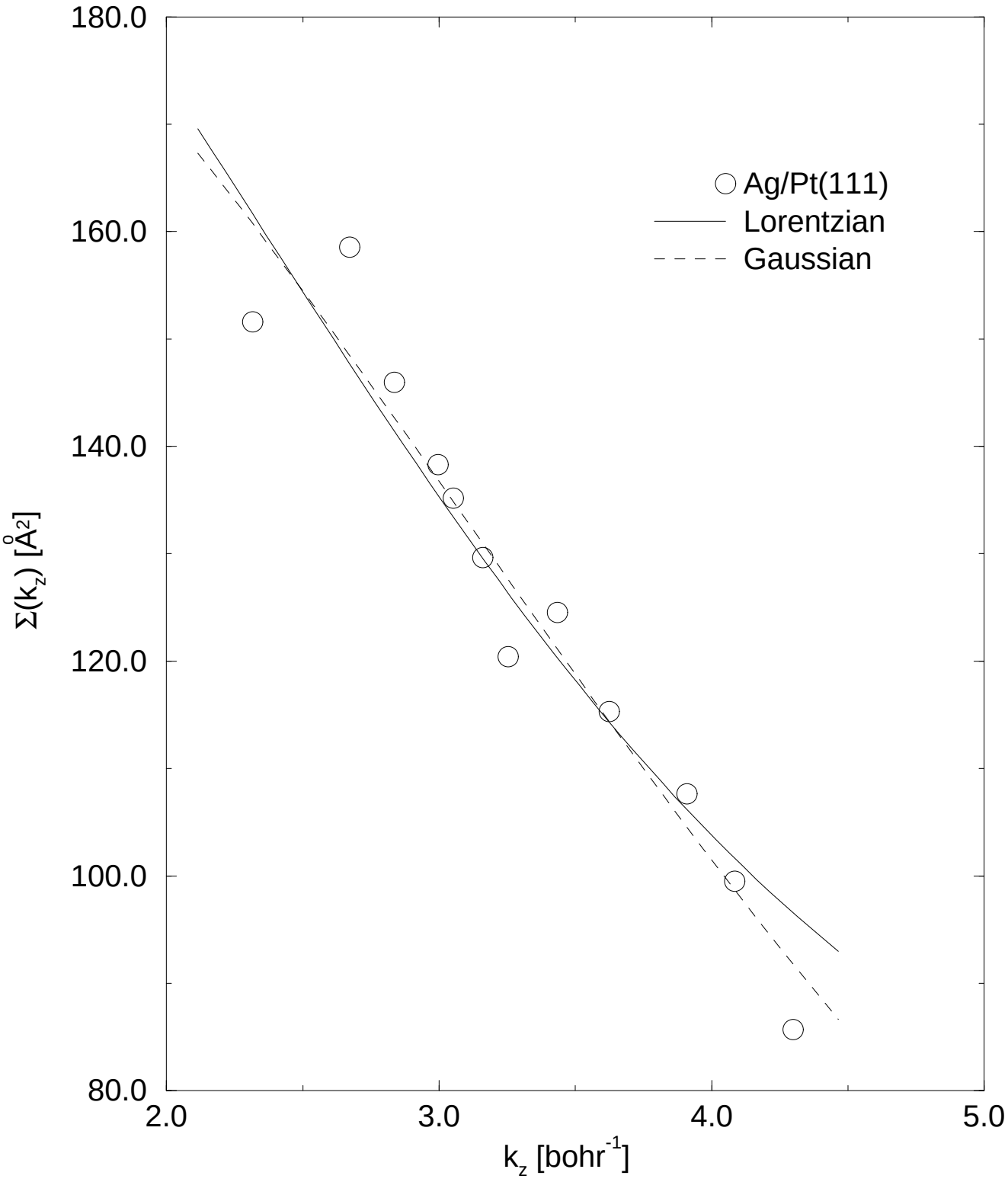
180.0
160.0
140.0
120.0
100.0
80.0
2.0
3.0
4.0
5.0
Σ(k_z) [Å^2]
k_z [bohr^-1]
Ag/Pt(111)
Lorentzian
Gaussian

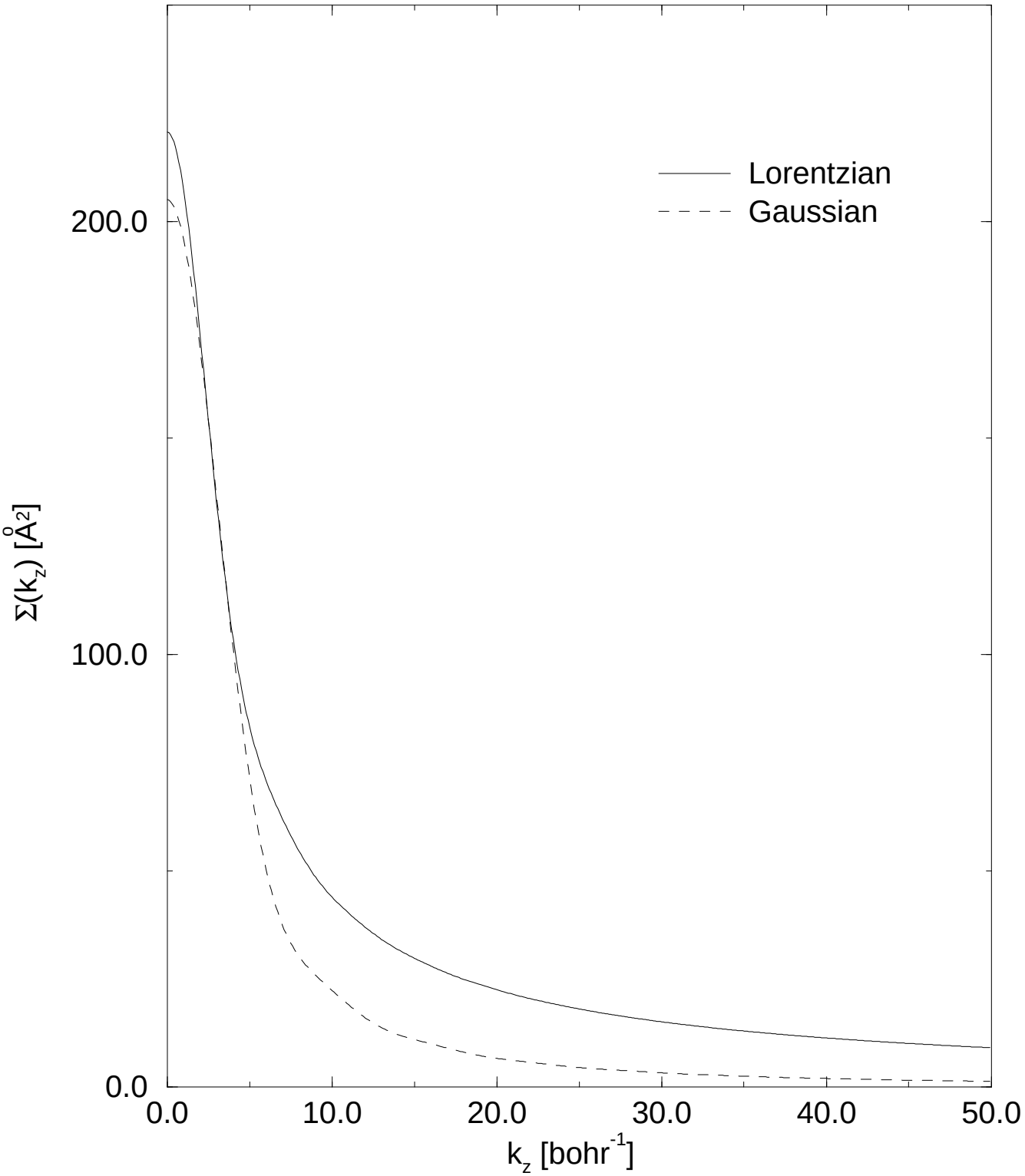
Lorentzian
Gaussian
200.0
100.0
0.0
0.0
10.0
20.0
30.0
40.0
50.0
Σ(k_z) [Å^2]
k_z [bohr^-1]

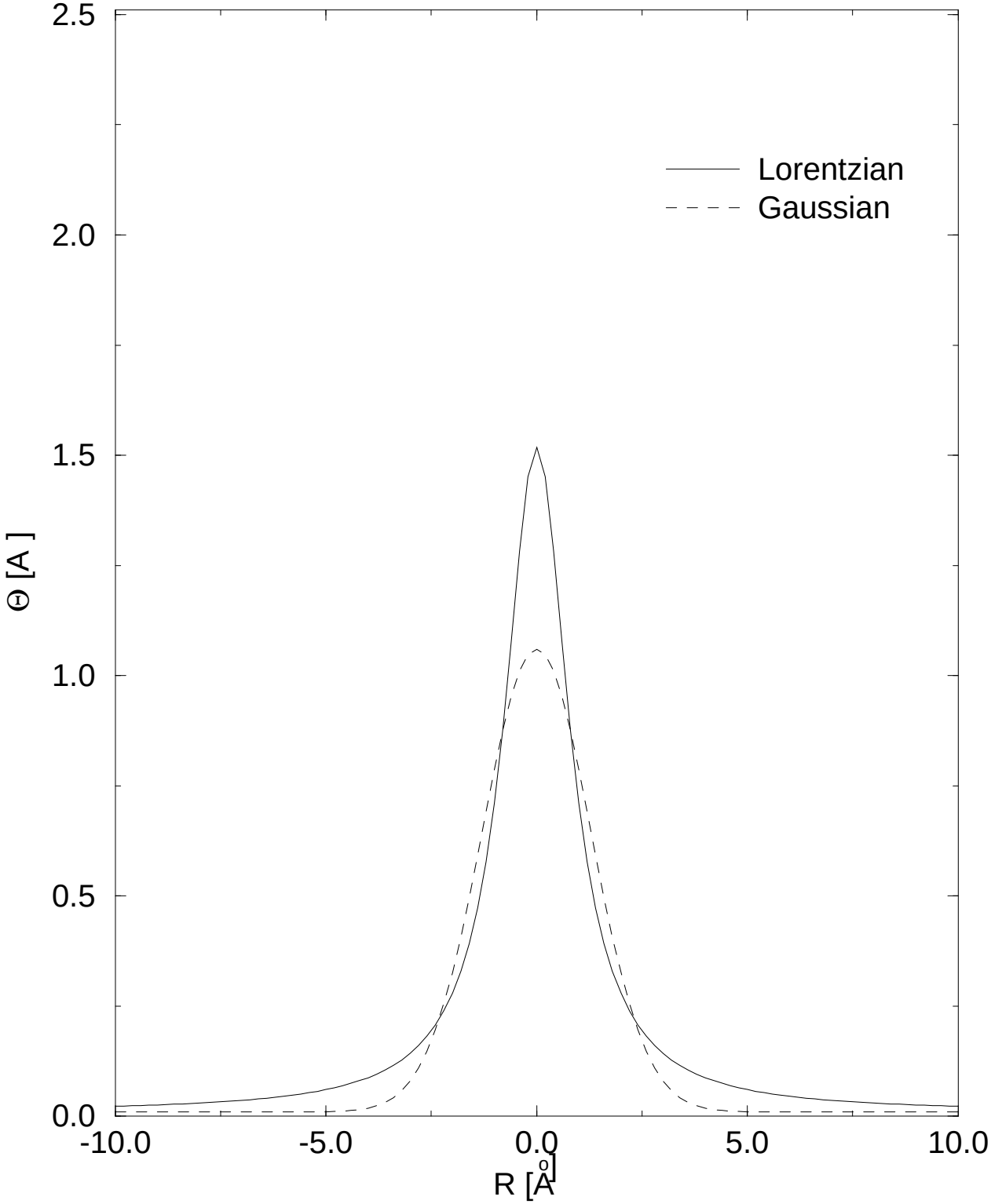
2.5
2.0
1.5
1.0
0.5
0.0
-10.0
-5.0
0.0
5.0
10.0
Lorentzian
Gaussian
Θ [A°]
R [A°]